IOSR Journal of Mathematics (IOSR-JM)
e-ISSN: 2278-5728, p-ISSN: 2319-765X. Volume 16, Issue 5 Ser. V (Sep. – Oct. 2020), PP 34-43
www.iosrjournals.org

Dissipative Heat Transfer on Hydromagnetic Flow of Copper and Alumina Ethylene-Glycol Based Nanofluid Over A Heated Vertical Plate

E. Mwaighacho, W. N. Mutuku
(Department of Mathematics and Actuarial Science, Kenyatta University, Kenya)

Abstract:*The cooling systems of automobiles influence the design of the frontal part of a car, the fuel consumption and the performance of its engine. In this study, Ethylene-Glycol based nanofluids with copper and Alumina as the nanoparticles are considered as coolants. The steady viscous flow of the electrically conducting liquids is considered to be along a heated vertical plate which imitates the flow of a coolant in a car radiator. The transformed boundary layer equations are non-dimensionalized using appropriate similarity variables and solved using the fourth order Runge-Kutta method coupled with a shooting technique. The influence of pertinent parameters on velocity profile, temperature profile, concentration profile, skin friction and Nusselt number are investigated and the results analyzed graphically using MATLAB.The results obtained were in good agreement with the actual flow dynamics.Al_2O_3-Ethylene glycol based nanofluid had the highest skin friction while Cu-Ethylene glycol based nanofluid had higher heat and mass transfer rates.*

Key Word*: MHD; Dissipative; Nanofluid; similarity variable.*

Date of Submission: 26-10-2020 Date of Acceptance: 05-11-2020

I. Introduction

Heat transfer has extensive applications in cooling and heating of fluids in industrial processes. Some of these applications include electronic cooling and the heat exchangers. Since most of the engineering processes involves boundary layer flows, great research has been done including the analysis of the effects of thermal buoyancy on the laminar boundary layer while considering the flow past a vertical plate[1]. By considering a convective surface boundary condition, it was noted that increasing the Prandtl number and the Grashof number leads to a reduction of the thermal boundary layer thickness along the plate. [2]did the numerical solution of boundary layer flow equation with viscous dissipation effect along a flat plate while considering varying temperature. It was observed that an increase in temperature lead to an increase in Eckert number while for a fixed Prandtl number and increase in Eckert number lead to a decrease in heat transfer at the wall.[3]studied a mixed convection flow in a channel with temperature dependent viscosity and a flow reversal. They concluded that an increase in viscosity variation parameter increases both fluid velocity as well as the skin friction at the heated wall.

Due to the influence of magnetic field on boundary layer flow, [4] numerically studied the magnetohydrodynamic convection flow of heat and mass transfer past a plate considering viscous dissipation and internal heat generation. The result indicated that velocity decreases with an increase in magnetic field strength, Schmidt number and Prandtl number while the rate of heat transfer decreases with increase in Prandtl number, Eckert number and an increased Schmidt number. [5] extended the work of [4] by considering entropy generation within a porous channel with insulated walls subjected to a magnetic field. He concluded that an increase in entropy generation was due to an increase in Eckert number and Hartmann number. External magnetic force was noted to affect the porous heat storage systems efficiency at a greater magnitude. [6]studied the hydromagnetic flow of a rotating fluid past in the presence of chemical reaction and radiation. The flow was past a vertical plate and he considered the plate to be porous. The results showed that the concentration decreases with increase in the chemical reaction parameter while the temperature increases with an increase with the radiation parameter

Owing to the growing demand and use of machines, the cooling of the machines has always been a great concern. The enhancement of heating and cooling in the industrial processes has been embraced since the commonly used based fluids such as water, ethylene glycol and engine oil have low thermal conductivities making them less efficient in heat transfer. In the need of finding a fluid with better heat transfer abilities [7] came up with a new class of heat transfer fluids called nanofluids which were obtained by suspending metallic nanoparticles in convectional heat transfer fluids termed as base fluids. It was concluded that the presence of the nanoparticles greatly lead to an increase in the heat transfer capabilities of the fluids due to improved viscosity, diffusivity and thermal conductivity. [8]proposed that Brownian motion had very little effect on the thermal conductivity of the nanofluid. [9]investigated the transient forced convection in a fluid valve filled with Copper

Oxide-water nanofluid. Prandtl number was varied but the Reynolds number and solid volume fraction was fixed and concluded that the structure of the fluid flow and temperature field within the fluid valve depended significantly on time and the Copper oxide nanoparticles was most effective in enhancing heat transfer at the highest Prandtl value. [10]studied MHD laminar free convective boundary layer flows of an electrically conducting nanofluid over a solid stationery vertical plate. He concluded that there was an increase in the rate of heat and mass transfer and also an increase in the velocity and temperature distributions due to an increase in the Newtonian heating parameter. [11]did a numerical study of copper-water nanofluid through a stretching channel under slip effects considering different shapes of particles. The study revealed that thermal boundary layer thickness increases by increasing the solid volume fraction. [12]studied the effects of variable fluid properties on the boundary layer flow and heat transfer of a nanofluid over a horizontal surface where the effects of Brownian motion viscous dissipation and thermophoresis were considered. It was concluded that the effect of the Brownian motion and the thermophoresis parameters is to lower the wall-temperature gradient and to reduce the thickness of the nanoparticle volume fraction boundary layer for the case of Brownian motion parameter and to increase the thickness of the nanoparticle volume fraction boundary layer for the case of the Thermophoresis parameter.

Since there is an interaction of magnetic field in most industrial process, researchers resolved to studying the effects of applying magnetic field in a nanofluid flow. [13] studied the effect of interaction between the electrical conductivity of the convectional base fluid and that of the nanoparticles under the influence of magnetic field in a boundary layer flow with heat transfer over a convectively heated flat surface, it was also observed that the presence of nanoparticles greatly enhance the magnetic susceptibility of nanofluids as compared to the base fluids. [14]numerically investigated the heat transfer of variable properties of Alumina-Ethylene Glycol-water nanofluid in buoyancy driven convection where a rectangular plate was heated differently. The results were that as the volume fraction on nanoparticle increases deterioration in heat transfer occurred as compared to the base fluid heat transfer because of increase in viscosity as the volume fraction of the nanoparticle increased. [15]analyzed the hydromagnetic boundary layer flow and heat transfer of nanofluids and obtained that the presence of nanoparticles greatly enhanced the magnetic susceptibility of nanofluids as compared to the convectional based fluids. On increasing the magnetic strength of the fluid velocity was decreased while the thermal boundary layer thickness was increased hence an increase in the surface cooling effect. [16]did a numerical study of electromagnetic flow and heat transfer characteristics of nanofluid inside a parallel plate micro channel. The nanofluid was actuated by Lorentz force and the influence of viscous dissipation and joule heating was also considered. It was noted that an increase of the joule parameter and Brinkman number lead to a decrease in heat transfer performance while an increase in nanoparticle volume fraction lead to an increase in heat transfer capabilities. The choice of the base fluid is of importance as different fluids have different properties. Glycol based fluids always lower the freezing point of water and prevent ice formation and also raises the boiling point of water when mixed together. This implies that the glycol based fluids can be used both in the cooling systems like refrigeration and in the heating systems like the car radiators and the industrial heat exchangers [17].

The aim of this study is to extend the work of [18] by considering the effects of mass transfer in the heat transfer abilities of copper and Alumina Ethylene-Glycol based nanofluid over a vertical heated plate since most industrial processes involve both the heat and the mass transfer. In the succeeding sections, the well-known boundary layer partial differential equations are transformed into nonlinear ordinary differential equations then later solved numerically by employing the shooting technique coupled with the fourth order Runge-Kutta method. The influence of pertinent parameters on the flow are analysed graphically and the results discussed

II. Problem Formulation

A steady two dimensional boundary layer flow of a nanofluid over a flat vertical plate is considered in this study. As shown in figure 1, the nanofluid flows across vertical surface (i.e. $x-$axis) while a magnetic field of strength B_0 is applied normal to the surface. The surface is subjected to Newtonian heating boundary conditions.

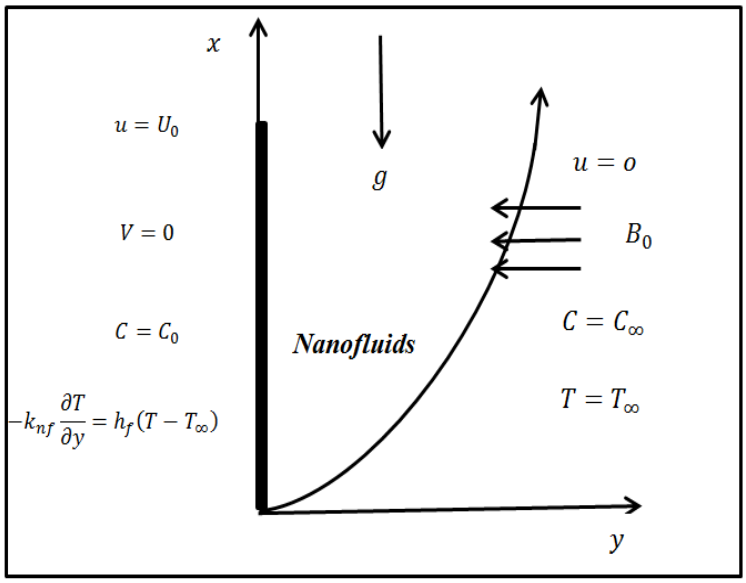

Figure 1: Flow configuration

By adding the Boussinesq approximation, the boundary layer equations are:

$$\frac{\partial u}{\partial x}+\frac{\partial v}{\partial y}=0 \tag{1}$$

$$u\frac{\partial u}{\partial x}+v\frac{\partial u}{\partial y}=\frac{\mu_{nf}}{\rho_{nf}}\frac{\partial^2 u}{\partial y^2}+\beta_{nf}\,g(T-T_\infty)-\frac{\sigma_{nf}B_0^2 u}{\rho_{nf}} \tag{2}$$

$$u\frac{\partial T}{\partial x}+v\frac{\partial T}{\partial y}=\frac{k_{nf}}{(\rho c_p)_{nf}}\frac{\partial^2 T}{\partial y^2}+\frac{\mu_{nf}}{(\rho c_p)_{nf}}\left(\frac{\partial u}{\partial y}\right)^2+\frac{\sigma_{nf}B_0^2u^2}{(\rho c_p)_{nf}} \tag{3}$$

$$u\frac{\partial C}{\partial x}+v\frac{\partial C}{\partial y}=D_B\frac{\partial^2 C}{\partial y^2} \tag{4}$$

Where (u,v) are the velocity componentsof the nanofluid in the (x,y) directions respectively, T is the temperature of the nanofluid, T_∞ is the free stream temperature, C is the concentration of the nanofluid,μ represents the dynamic viscosity, ρ the density, β denotes the thermal expansion coefficient, B_o stands for magnetic field, σ stands for electrical conductivity of the nanofluid, k is the thermal conductivity, ρc_p refers to heat capacitance of the fluid, D_B represents the Brownian diffusion coefficient and the subscripts nf stand for nanofluids.

According to [14], the following constant properties were validated experimentally by various researchers in relation between the nanofluid (*nf*), the base fluid (*bf*) and the nanoparticles (*np*). These relations can be used to determine the physical properties of nanofluids such as density, viscosity, specific heat, volume expansion and thermal conductivity at different temperatures and concentrations.

$$\begin{aligned}
\rho_{nf} &= (1-\varphi)\rho_{bf}+\varphi\rho_{np}\\
\mu_{nf} &= \frac{\mu_{bf}}{(1-\varphi)^{2.5}}\\
\beta_{nf} &= (1-\varphi)\beta_{bf}+\varphi\beta_{np}\\
(\rho c_p)_{nf} &= (1-\varphi)(\rho c_p)_{bf}+\varphi(\rho c_p)_{np}\\
k_{nf} &= \frac{k_{np}+2k_{bf}-2\varphi(k_{bf}-k_{np})}{k_{np}+2k_{bf}+\varphi(k_{bf}-k_{np})}k_{bf}\\
\sigma_{nf} &= (1-\varphi)\sigma_{bf}+\varphi\sigma_{np}
\end{aligned} \tag{5}$$

The boundary conditions at the plate surface and at the free stream may be written as

$$u(x,0)=U_0,\qquad v(x,0)=0,\qquad -k_{nf}\frac{\partial T}{\partial y}(x,0)=h_f\left(T_f-T(x,0)\right)$$
$$C(x,0)=C_0$$
$$u(x,\infty)=0,\qquad T(x,\infty)\to T_\infty,\qquad C(x,\infty)\to C_\infty \tag{6}$$

whereC_w and C_∞ the nanoparticle concentration at the wall and at the free stream respectively.
Introducing the stream function $\psi(x,y)$ which satisfies the continuity Equation 1

$$u = \frac{\partial \psi}{\partial y}, \quad v = -\frac{\partial \psi}{\partial x} \tag{7}$$

In order to simplify Equations 1-6, we introduce the similarity variableη, the non-dimensional stream function$f(\eta)$, the non-dimensional temperature$\theta(\eta)$, the non-dimensional concentration$\phi(\eta)$. The transformations are

$$\eta = \left(\frac{a}{\nu_{bf}}\right)^{\frac{1}{2}} y, \qquad \psi = \left(\sqrt{av}\right) x f(\eta), \qquad \theta(\eta) = \frac{T - T_\infty}{T_w - T_\infty}, \qquad \phi(\eta) = \frac{C - C_\infty}{C_w - C_\infty} \tag{8}$$

Substituting Equations (7) and (8) into Equations 1-6, we obtain the following system of ordinary equations

$$f''' + Gr\theta - Mf' + ff'' - (f')^2 = 0 \tag{9}$$
$$A\theta'' + PrEc(f'')^2 + MEcPr(f')^2 + Pr\theta' = 0 \tag{10}$$
$$\phi'' + Scf\phi' = 0 \tag{11}$$

Subject to the boundary conditions

$$\text{at } \eta = 0; \ f' = 1, \ \ f = 0, \ \ \theta' = Bi(\theta - 1), \ \ \phi = 1 \tag{12}$$
$$\text{as } \eta \to \infty; \ f' = 0, \qquad \theta \to 0, \qquad \phi \to 0 \tag{13}$$

Where prime represents the differentiation with respect to η and

$$Gr = \frac{\beta_{nf}\, g(T_W - T_\infty)}{a^2 x}, M = \frac{\sigma_{nf} B_0^2}{a\rho_{nf}}, Pr = \frac{\mathrm{U}_{nf}}{\alpha_{bf}}, Ec = \frac{a^2 x^2}{(c_p)_{nf}(T_w - T_\infty)},$$

$$, Sc = \frac{\mathrm{U}_{nf}}{D_B}, Bi = \frac{h}{k_{nf}}\left(\frac{\mathrm{U}_{nf}}{a}\right)^{1/2}$$

represents the Grashof Number, Magnetic field Parameter, Prandtl Number, Eckert Number, and the Schmidt Number and the local Biot number respectively.

III. Results and Discussion

The non-linear ordinary equations 9-11 are numerically solved using MATLAB while considering their boundary conditions 12-13. The thermophysical properties for Copper and Alumina nanoparticles together with Ethylene Glycol as the base fluids are considered and the values represented in table 1 below.

Table 1: Thermophysical properties of Ethylene-glycol and the nanoparticles

Materials	Density ρ (kg/m^3)	Specific heat at constant pressure c_p (J/kgK)	Thermal conductivity k (W/mK)	Electrical conductivity σ (S.m^{-1})	Thermal expansion coefficients β(K^{-1})	Dynamic Viscosityμ (pa.s)
Ethylene- glycol	1114	2415	0.252	1.07×10^{-6}	6.5×10^{-5}	0.0161
Alumina (Al_2O_3)	3970	765	40	3.69×10^{7}	0.85×10^{-5}	_
Copper (Cu)	8933	385	401	5.96×10^{7}	1.67×10^{-5}	_

The effects of pertinent parameters on velocity, temperature and concentration profiles are represented graphically and the effects on skin friction are tabulated as shown below.

Dimensionless velocity profiles

Figures 2-7 show the effects of various physical parameters on the primary and the secondary velocity profiles of the nanofluids. For the case of the primary velocity, it is noted that the velocity is maximum at the plate surface but gradually decreases to zero at the ambient area far away from the plate with regards to all pertinent parameters, thus satisfying the boundary conditions. Consequently the secondary velocity is observed to increase gradually from zero close to the plate attaining a maximum velocity at the free stream. In figure 2, an increase in magnetic parameter leads to a decrease in the fluid velocity. This is due to an increase in the Lorentz force, a resistive force which tends to retard the motion of the fluid. An increase in the viscous dissipation parameter (Ec), leads to an increase in the velocity of the fluid as shown in figure 4. Figure 6 shows the effects

of increasing Grashof number on velocity profiles. An increase in the Grashof number results to the increase in velocity due to buoyancy forces.

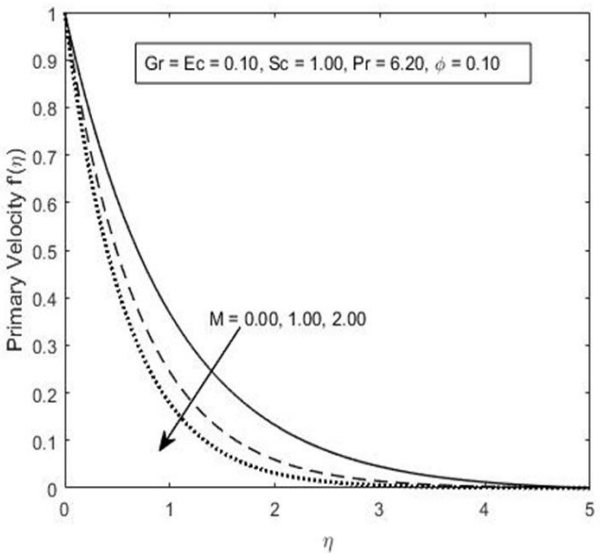

Figure 2: Primary velocity profile for increasing magnetic field parameter

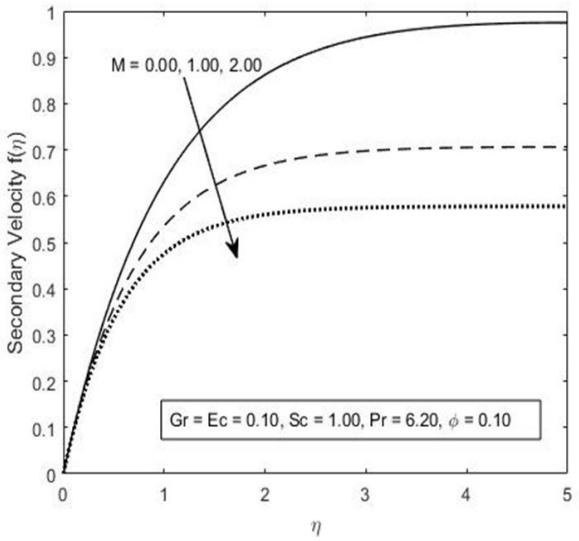

Figure 3: Secondary velocity profile for increasing magnetic field parameter

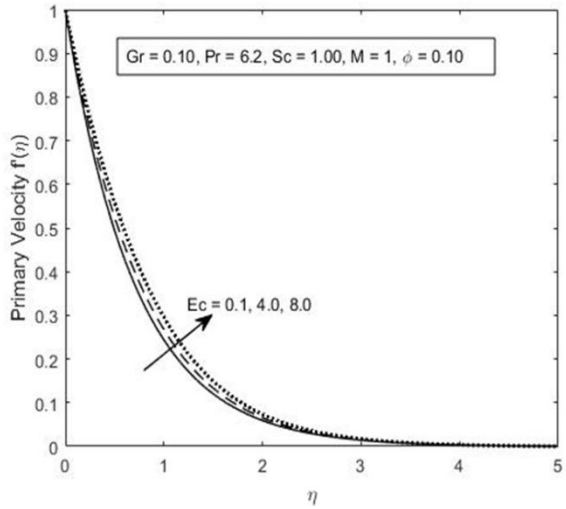

Figure 4: Primary velocity profile for increasing Eckert number

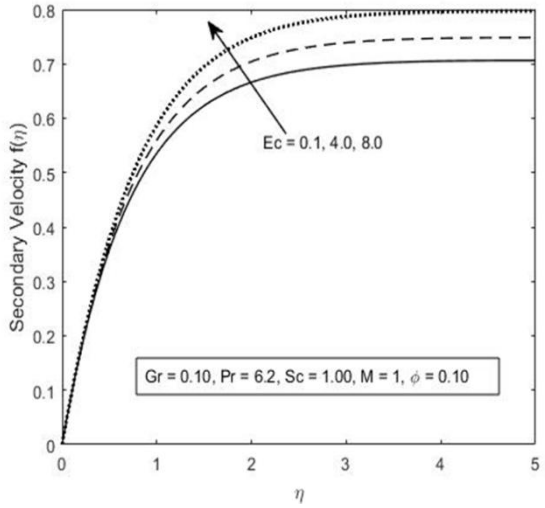

Figure 5: Secondary velocity profile for increasing Eckert number

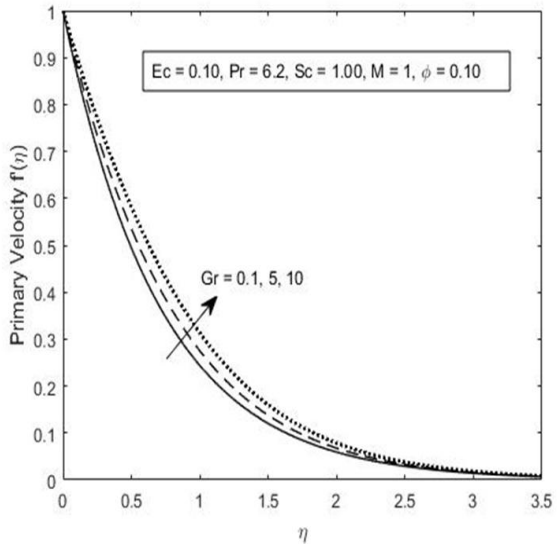

Figure 6: Primary velocity profile for increasing Grashof number

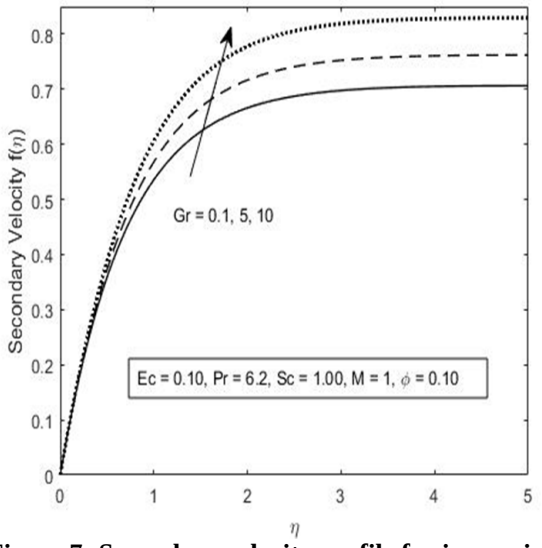

Figure 7: Secondary velocity profile for increasing Grashof number

Dimensionless Temperature Profiles

Figures 8-12 illustrates the fluid temperature profiles within the boundary layer. It can be observed that the fluid temperature is highest at the plate surface and decreases exponentially to zero at the free stream area far away from the plate satisfying the boundary conditions. From these figures, the thermal boundary layer thickness increases with an increase in the Magnetic field parameter, Eckert number and the local Biot number while it decreases with an increase in the Prandtl number. An increase in Magnetic parameter would result in an increase in the induced Lorentz force which will lead to resistance to the flow of the fluid as discussed in fig 2. Consequently this will result in an increase in the temperature as depicted in fig 8. An increase in the local Biot number leads to an increased rate at which heat is transferred between the hot plate and the fluid while an increase in Eckert number results in increase in temperatures due to the additional heating caused by the viscous dissipation. Since the Prandtl number is the ratio of viscous diffusion to thermal diffusion, an increase in Prandtl number would result in a decrease in the thermal boundary layer thickness hence a decrease in the temperature. Figure 12 shows the variation of Grashof number to the temperature profiles. An increase in Grashof number reduces the thermal boundary layer but at the free stream the temperature is seen to rise with increase in Grashof number.

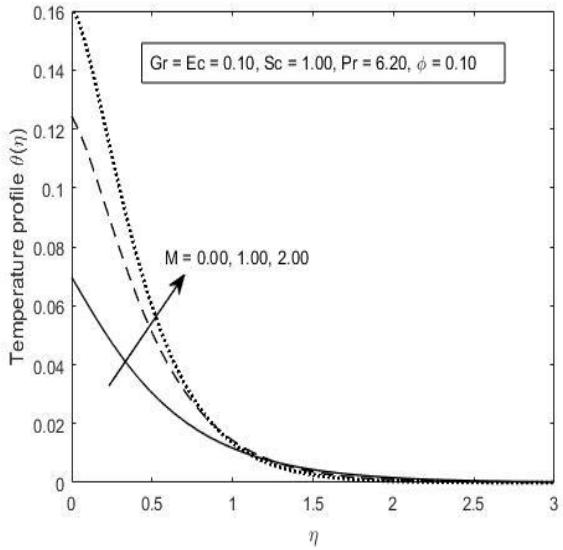

Figure 8: Temperature profile for increasing magnetic field parameter

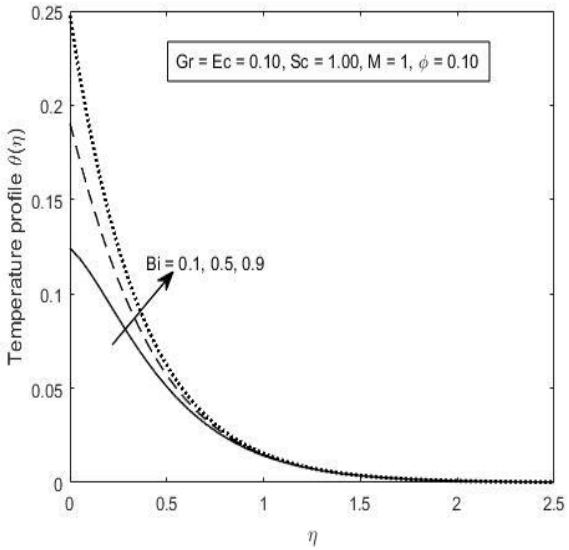

Figure 9: Temperature profile for increasing Local Biot number

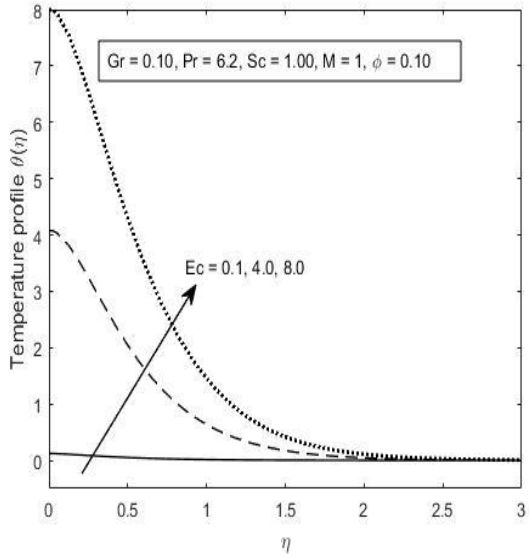

Figure 10: Temperature profiles for increasing Eckert number

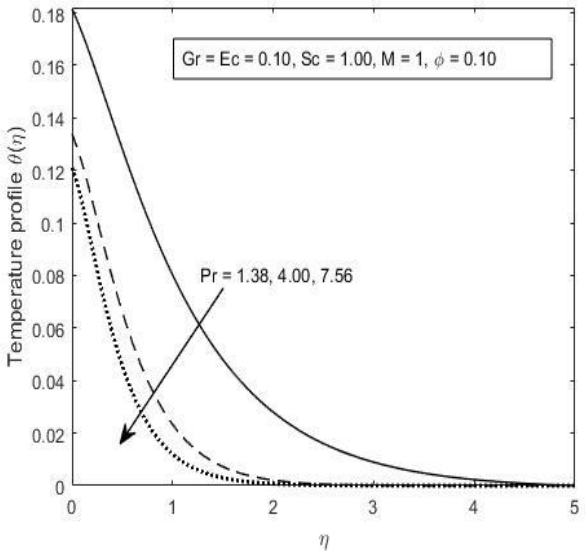

Figure 11: Temperature profile for increasing Prandtl number

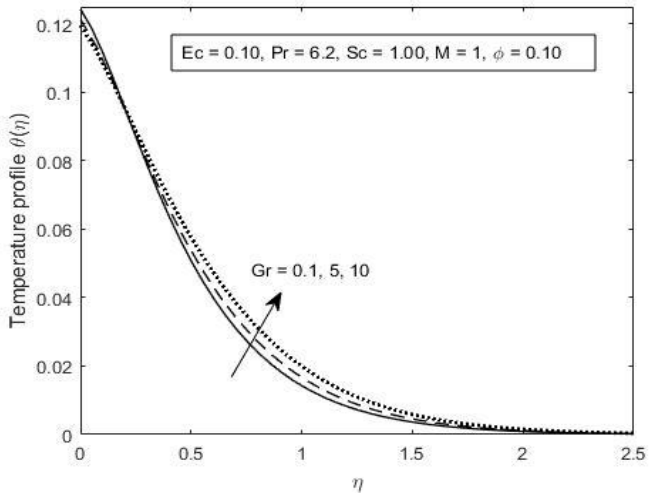

Figure 12: Temperature profiles for increasing Grashof number

Dimensionless Concentration Profiles

Fig 13-16 shows the concentration profiles against the span wise coordinate η for varying values of Magnetic parameter, Eckert number, Schmidt number and the Grashof number. The species concentration is seen to decrease to zero from the late surface up to a region far away from the plate, thus satisfying the boundary conditions. From these figures, it can be noted that varying the magnetic field parameter and the Schmidt number have great influence to the concentration boundary layer while changes in the Eckert number has very little effect to the species concentration gradient. Fig 13 shows that increasing the Magnetic field parameter leads to an increase in concentration gradient. This is due to the resistive force induced which will in turn reduce the velocity and subsequently increase the temperature of the fluid. An increase in the temperature of the fluid will increase the diffusion coefficient of the nanofluids hence increase in the concentration gradient. Fig 15 depicts that an increase in Schmidt number leads to a decrease in concentration due to a weaker solute diffusivity leading to a shallower penetration of solutal effect. Figure 16 shows that an increase in the Grashof number would result to a decrease in the concentration. This is because an increase in buoyancy forces leads to a further dispersion of the concentration species.

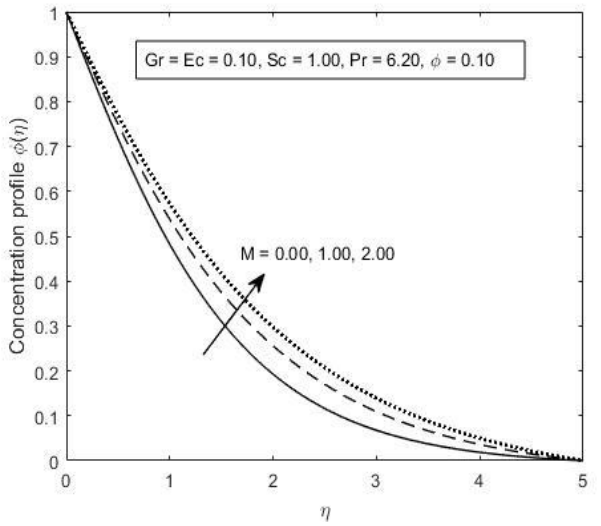

Figure 13: Concentration profiles for increasing magnetic field parameter

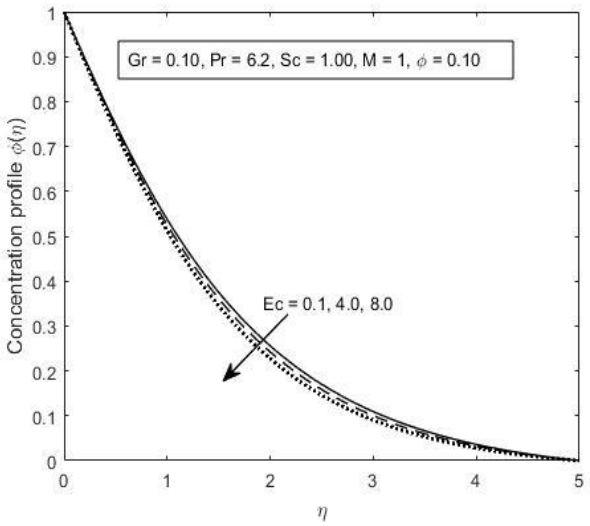

Figure 14: Concentration profile for increasing Eckert number

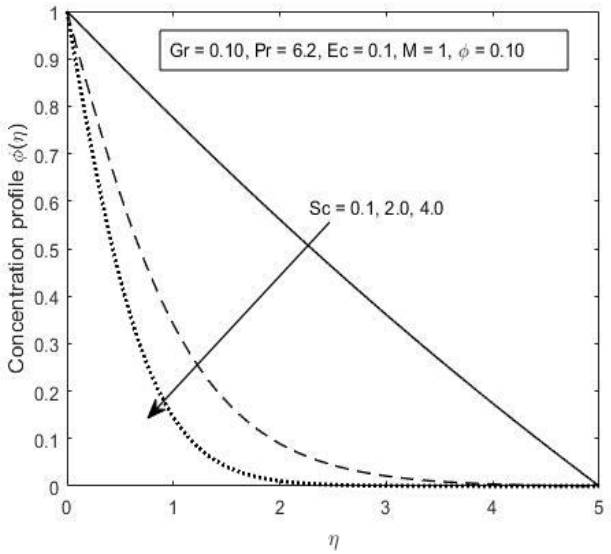

Figure 15: Concentration profile for increasing Schmidt number

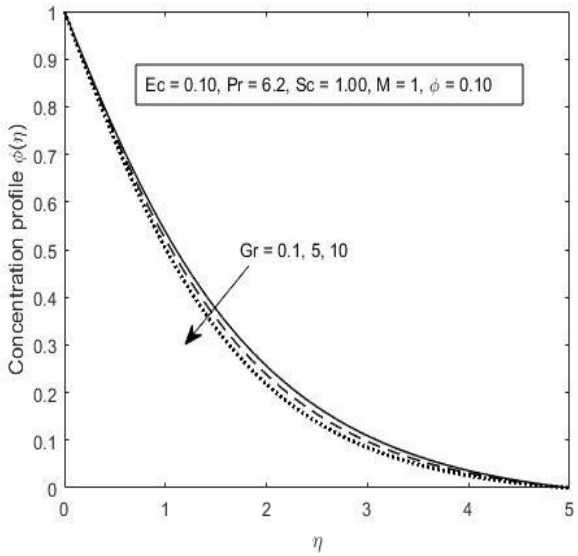

Figure 16: Concentration profile for increasing Grashof number

Effects of variation of parameters on Skin friction, Nusselt number and Sherwood number on the two nanofluids.

The tables below shows values of Skin friction coefficient (Cf), Nusselt number (Nu) and Sherwood number (Sh) when varying the Grashof number and the Eckert number while considering the two nanofluids. Table 2 shows the effects of increasing the buoyancy forces leads to an increase in the skin friction and the Nusselt number but a decrease of the Sherwood number. The Al_2O_3-Ethylene Glycol nanofluid is showing a faster growth in the skin friction as compared to the Cu-Ethylene Glycol nanofluid. The Nusselt number is increasing at the same rate for both nanofluids while the Sherwood number is decreasing at the same rate for both nanofluids too. Table 3 below shows that an increase in the Eckert number leads to an increase in the skin friction and a decrease in both the Nusselt number and the Sherwood number. The skin friction is seen to increase gradually for both nanofluids. The rate of heat transfer is seen to decrease rapidly when the Eckert number is increased. Increasing both the Grashof number and the Eckert number leads to a faster growth of the skin friction while the rate of heat transfer and mass transfer decreased at a faster rate as compared to when the parameters were varied independently. Al_2O_3-Ethylene Glycol based nanofluids showed a faster increase of the skin friction, while the Nusselt number and the Sherwood number varied at the same rate for both nanofluids.

Table 2: Effects of varying Grashof number on skin friction, Nusselt number and Sherwood number

Gr	Ec	Sc	Pr	phi	cpnp	Nanoparticle	Cf	Nu	Sh
0.1	0.1	1	6.2	0.1	385	Cu	-1.41038	0.08757	-0.51928
0.1	0.1	1	6.2	0.1	765	Al2O3	-1.41037	0.08755	-0.51929
0.2	0.1	1	6.2	0.1	385	Cu	-1.40653	0.08758	-0.51968
0.2	0.1	1	6.2	0.1	765	Al2O3	-1.4065	0.08756	-0.51968
0.4	0.1	1	6.2	0.1	385	Cu	-1.39881	0.08759	-0.52047
0.4	0.1	1	6.2	0.1	765	Al2O3	-1.39876	0.08757	-0.52048
0.6	0.1	1	6.2	0.1	385	Cu	-1.39109	0.0876	-0.52127
0.6	0.1	1	6.2	0.1	765	Al2O3	-1.39101	0.08759	-0.52128
0.8	0.1	1	6.2	0.1	385	Cu	-1.38336	0.08762	-0.52207
0.8	0.1	1	6.2	0.1	765	Al2O3	-1.38325	0.0876	-0.52209
1	0.1	1	6.2	0.1	385	Cu	-1.37563	0.08763	-0.52287
1	0.1	1	6.2	0.1	765	Al2O3	-1.37549	0.08761	-0.52289

Table 3: Effects of varying the Eckert number to skin friction, Nusselt number and the Sherwood number

Gr	Ec	Sc	Pr	phi	cpnp	Nanoparticle	Cf	Nu	Sh
0.1	0.1	1	6.2	0.1	385	Cu	-1.41038	0.08757	-0.51928
0.1	0.1	1	6.2	0.1	765	Al2O3	-1.41037	0.08755	-0.51929
0.1	0.2	1	6.2	0.1	385	Cu	-1.40685	0.0772	-0.51966
0.1	0.2	1	6.2	0.1	765	Al2O3	-1.40683	0.07718	-0.51967
0.1	0.4	1	6.2	0.1	385	Cu	-1.39978	0.0565	-0.52042
0.1	0.4	1	6.2	0.1	765	Al2O3	-1.39974	0.05649	-0.52043
0.1	0.6	1	6.2	0.1	385	Cu	-1.3927	0.03585	-0.52118
0.1	0.6	1	6.2	0.1	765	Al2O3	-1.39265	0.03585	-0.5212
0.1	0.8	1	6.2	0.1	385	Cu	-1.38562	0.01526	-0.52195
0.1	0.8	1	6.2	0.1	765	Al2O3	-1.38555	0.01526	-0.52196
0.1	1	1	6.2	0.1	385	Cu	-1.37853	-0.528	-0.52271
0.1	1	1	6.2	0.1	765	Al2O3	-1.37844	-0.528	-0.52274

Table 4: effects of varying both the Eckert number and the Grashof number on skin friction, Nusselt number and the Sherwood number

Gr	Ec	Sc	Pr	phi	cpnp	Nanoparticle	Cf	Nu	Sh
0.1	0.1	1	6.2	0.1	385	Cu	-1.41038	0.08757	-0.51928
0.1	0.1	1	6.2	0.1	765	Al2O3	-1.41037	0.08755	-0.51929
0.2	0.2	1	6.2	0.1	385	Cu	-1.39946	0.07723	-0.52044
0.2	0.2	1	6.2	0.1	765	Al2O3	-1.39941	0.07721	-0.52045
0.4	0.4	1	6.2	0.1	385	Cu	-1.35626	0.05681	-0.52509
0.4	0.4	1	6.2	0.1	765	Al2O3	-1.35611	0.0568	-0.52512
0.6	0.6	1	6.2	0.1	385	Cu	-1.28408	0.03694	-0.53306
0.6	0.6	1	6.2	0.1	765	Al2O3	-1.28376	0.03693	-0.53314
0.8	0.8	1	6.2	0.1	385	Cu	-1.18122	0.01768	-0.54485
0.8	0.8	1	6.2	0.1	765	Al2O3	-1.18067	0.01769	-0.54498
1	1	1	6.2	0.1	385	Cu	-1.04321	-0.00121	-0.5614
1	1	1	6.2	0.1	765	Al2O3	-1.04236	-0.0012	-0.56161

IV. Conclusion

This paper investigates the dissipative heat transfer on hydromagnetic flow of Ethylene-Glycol based nanofluids containing two different nanoparticles (Copper and Alumina) while considering the flow on a vertical plate. Based on numerical analysis and the graphical presentations, the following conclusions were made;

- Velocity profiles increases with increase in Eckert number and Grashof number but decreases with increase in Magnetic field parameter, Variations of the Schmidt number, Prandtl number and the local Biot number have no effects to the momentum boundary layer.
- Temperature profiles increases with increase in the Eckert number, Magnetic field parameter, Grashof number and the local Biot number while decreases with increase in the Prandtl number, Schmidt number has no effects in the thermal boundary layer.
- Concentration profiles increases with increase in Magnetic field parameter, but decreases with increase Eckert number, Schmidt number and the Grashof number. The local Biot number and the Prandtl number had no effect to the concentration boundary layer.
- Variation of Grashof number led to an increase in both the skin friction and the Nusselt number while a decrease in the Sherwood number. Variation of the Eckert number led to an increase of the skin friction but a decrease of both the Nusselt number and the Sherwood number.
- When both the Grashof number and the Eckert number were varied with equal values, an increase in the skin friction and a decrease in the Nusselt number and the Sherwood number were noted. This showed that the viscous forces were more dominant over the buoyancy forces.
- Al_2O_3-Ethylene glycol based nanofluid had the highest skin friction while Cu-Ethylene glycol based nanofluid had higher heat and mass transfer rates.
- From engineering point of view, Cu-EG would make the best coolant due to its higher rate of heat transfer caused by a higher mass flow rate and that it causes less tear and wear on the plate surface due to minimal skin friction.
- Enhancement of metal nanoparticles in base fluids produces better coolants as compared to the use of metal oxides nanoparticles.

References

[1] O. D. Makinde and P. O. Olanrewaju, "Buoyancy Effects on Thermal Boundary Layer Over a Vertical Plate With a Convective Surface Boundary Condition," vol. 132, no. April, pp. 1–4, 2010, doi: 10.1115/1.4001386.

[2] S. Desale and V. H. Pradhan, "Numerical Solution of Boundary Layer Flow Equation with Viscous Dissipation Effect Along a Flat Plate with Variable Temperature," *Procedia Eng.*, vol. 127, pp. 846–853, 2015, doi: 10.1016/j.proeng.2015.11.421.

[3] B. K. Jha, M. O. Oni, and B. Aina, "Steady fully developed mixed convection flow in a vertical micro-concentric-annulus with heat generating/absorbing fluid: An exact solution," *Ain Shams Eng. J.*, vol. 9, no. 4, pp. 1289–1301, 2018, doi: 10.1016/j.asej.2016.08.005.

[4] K. B. Lakshmi, G. S. S. Raju, P. M. Kishore, and N. V. R. V. P. Rao, "The Study of Heat Generation and Viscous Dissipation on Mhd Heat And Mass Diffusion Flow Past A Surface," vol. 5, no. 4, pp. 17–28, 2013.

[5] B. Amami, H. Dhahri, and A. Mhimid, "Viscous dissipation effects on heat transfer, energy storage, and entropy generation for fluid flow in a porous channel submitted to a uniform magnetic field," no. February 2016, 2014, doi: 10.1615/JPorMedia.v17.i10.10.

[6] S. Sivaiah, "MHD flow of a rotating fluid past a vertical porous flat plate in the presence of chemical reaction and radiation," *J. Eng. Phys. Thermophys.*, vol. 86, no. 6, pp. 1328–1336, 2013, doi: 10.1007/s10891-013-0957-1.

[7] C. Stephen and Eastman J.A., "Enhancing thermal conductivities of fluids using nanoparticles.pdf." .

[8] W. Evans and J. Fish, "Role of Brownian motion hydrodynamics on nanofluid thermal conductivity," pp. 3–5, 2006, doi: 10.1063/1.2179118.

[9] R. Nasrin, M. A. Alim, and A. J. Chamkha, "Prandtl number variation on transient forced convection flow in a fluid valve using nanofluid," vol. 4, no. 2, pp. 1–16, 2012.

[10] M. J. Uddin, W. A. Khan, and A. I. Ismail, "MHD Free Convective Boundary Layer Flow of a Nanofluid past a Flat Vertical Plate with Newtonian Heating Boundary Condition," vol. 7, no. 11, pp. 1–8, 2012, doi: 10.1371/journal.pone.0049499.

[11] J. Raza, A. M. Rohni, and Z. Omar, "Numerical Investigation of Copper-Water (Cu-Water) Nanofluid with Different Shapes of Nanoparticles in a Channel with Stretching Wall : Slip Effects," 2016, doi: 10.3390/mca21040043.

[12] K. V Prasad, "HEAT TRANSFER PHENOMENA IN A MOVING NANOFLUID OVER A HORIZONTAL SURFACE," vol. 28, no. 3, pp. 579–588, 2019.

[13] O. D. Makinde, W. N. Mutuku, and I. Studies, "HYDROMAGNETIC THERMAL BOUNDARY LAYER OF NANOFLUIDS OVER A CONVECTIVELY HEATED FLAT PLATE WITH VISCOUS DISSIPATION AND OHMIC HEATING," vol. 76, no. 0, 2014.

[14] H. Khorasanizadeh, M. M. Fakhari, and S. P. Ghaffari, "Investigation of Heat Transfer Enhancement or Deterioration of Variable Properties Al 2 O 3 -EG-water Nanofluid in Buoyancy Driven Convection," vol. 2, no. 1, pp. 48–64, 2014, doi: 10.7508/tpnms.2014.01.005.

[15] W. N. Mutuku, "ANALYSIS OF HYDROMAGNETIC BOUNDARY LAYER FLOW AND HEAT," no. January, 2014.

[16] P. Zhao, J. Jian, and Q. Li, "ELECTROMAGNETOHYDRODYNAMIC FLOW AND HEAT TRANSFER OF NANOFLUID IN A PARALLEL PLATE MICROCHANNEL," *J. Mech.*, vol. 33, no. 1, pp. 155–124, 2019.

[17] G. Sekrani and S. Poncet, "applied sciences Ethylene- and Propylene-Glycol Based Nanofluids : A Litterature Review on Their Thermophysical Properties and Thermal Performances," 2018, doi: 10.3390/app8112311.

[18] W. N. Mutuku, "Ethylene glycol (EG)- based nanofluids as a coolant for automotive radiator," *Asia Pacific J. Comput. Eng.*, pp. 1–15, 2016, doi: 10.1186/s40540-016-0017-3.